Inorg. Chem. **2000,** *39,* 304−307

Mechanism of CO Exchange on *cis*-$[M(CO)_2X_2]^-$ Complexes (M = Rh, Ir; X = Cl, Br, or I)[1]

Raphaël Churlaud, Urban Frey, François Metz,[†] and André E. Merbach*

Institut de Chimie Minérale et Analytique, Université de Lausanne, BCH,
CH-1015 Lausanne, Switzerland

Received September 8, 1999

The CO exchange on *cis*-$[M(CO)_2X_2]^-$ with M = Ir (X = Cl, **1a**; X = Br, **1b**; X = I, **1c)** and M = Rh (X = Cl, **2a**; X = Br, **2b**; X = I, **2c**) was studied in dichloromethane. The exchange reaction [*cis*-$[M(CO)_2X_2]^-$ + 2*CO $\rightleftarrows$ *cis*-$[M({}^*CO)_2X_2]^-$ + 2CO (exchange rate constant: k_{obs})] was followed as a function of temperature and carbon monoxide concentration (up to 6 MPa) using homemade high gas pressure NMR sapphire tubes. The reaction is first order for both CO and *cis*-$[M(CO)_2X_2]^-$ concentrations. The second-order rate constant, k_2^{298} ($=k_{obs}$/[CO]), the enthalpy, $\Delta H^{\ddagger}$, and the entropy of activation, $\Delta S^{\ddagger}$, obtained for the six complexes are respectively as follows: **1a**, $(1.08 \pm 0.01) \times 10^3$ L mol^{-1} s^{-1}, 15.37 ± 0.3 kJ mol^{-1}, −135.3 ± 1 J mol^{-1} K^{-1}; **1b**, $(12.7 \pm 0.2) \times 10^3$ L mol^{-1} s^{-1}, 13.26 ± 0.5 kJ mol^{-1}, −121.9 ± 2 J mol^{-1} K^{-1}; **1c**, $(98.9 \pm 1.4) \times 10^3$ L mol^{-1} s^{-1}, 12.50 ± 0.6 kJ mol^{-1}, −107.4 ± 2 J mol^{-1} K^{-1}; **2a**, $(1.62 \pm 0.02) \times 10^3$ L mol^{-1} s^{-1}, 17.47 ± 0.4 kJ mol^{-1}, −124.9 ± 1 J mol^{-1} K^{-1}; **2b**, $(24.8 \pm 0.2) \times 10^3$ L mol^{-1} s^{-1}, 11.35 ± 0.4 kJ mol^{-1}, −122.7 ± 1 J mol^{-1} K^{-1}; **2c**, $(850 \pm 120) \times 10^3$ L mol^{-1} s^{-1}, 9.87 ± 0.8 kJ mol^{-1}, −98.3 ± 4 J mol^{-1} K^{-1}. For complexes **1a** and **2a**, the volumes of activation were measured and are −20.9 ± 1.2 cm^3 mol^{-1} (332.0 K) and −17.2 ± 1.0 cm^3 mol^{-1} (330.8 K), respectively. The second-order kinetics and the large negative values of the entropies and volumes of activation point to a limiting associative, A, exchange mechanism. The reactivity of CO exchange follows the increasing *trans* effect of the halogens ($Cl < Br \ll I$), and this is observed on both metal centers. For the same halogen, the rhodium complex is more reactive than the iridium complex. This reactivity difference between rhodium and iridium is less marked for chloride (1.5:1) than for iodide (8.6:1) at 298 K.

Introduction

The square-planar complexes *cis*-$[Rh(CO)_2X_2]^-$ and *cis*-$[Ir(CO)_2X_2]^-$ (X = halogen) are important intermediates in industrial catalytic cycles for carbonylation of alcohols or olefins to form carboxylic acids.[2−4] Although these reactions involving oxidative additions and substitutions have been widely studied,[5−11] to our knowledge, no kinetic data are available for carbonyl substitution in Rh(I) and Ir(I) square-planar complexes.

Kinetic data for substitution in square-planar complexes, including symmetric exchange reactions, are mainly available for Pd(II) and Pt(II) complexes,[12,13] and few examples are known for Rh(I),[14,15] Ir(I),[16] and Au(III) complexes.[17−19] The mechanism of substitution in square-planar complexes is well established.[12] Generally, it involves two parallel pathways: one is the direct attack of the nucleophile, whereas the other is the attack of the solvent in a first step. Both pathways show associative modes of activation. In weakly coordinating solvents, the solvent pathway is most often of negligible amplitude. However, it has been shown that organometallic Pt(II) substrates can substitute according to dissociative pathways.[20]

Free CO exchange on square-planar complexes has been reported only for $[M(CO)X_3]^-$ complexes (M = Pd, Pt; X = Cl, Br, I)[21] and for $[Rh_2(CO)_4Cl_2]$, $[Rh(P(C_6H_5)_3)_2COCl]$, and $[Pt_2(CO)_2Cl_4]$.[22] Another study, in the absence of free CO, proved intermolecular CO exchange between two complexes of Rh(I) or Ir(I).[16] This exchange proceeds via a five-coordinated dimeric intermediate with two bridged CO ligands. The studies on intermolecular exchange with free CO are rare because they require the use of CO pressure to have enough dissolved gas in

---

[†] Permanent address: Rhône-Poulenc Industrialisation, CRIT-Carrières, 85 avenue des frères Perret, 69192 St. Fons, France.

(1) *High-Pressure NMR Kinetics*. 90. For part 89 see: Caravan, P.; Toth, E.; Rockenbauer, A.; Merbach, A. E. *J. Am. Chem. Soc.* **1999**, *121*, 10403.
(2) Paulik, F. E.; Hershman, A.; Knox, W. R.; Roth, J. E.; Monti, D. (Monsanto Co.). *U.S. Patent 3,769,329*, 1973.
(3) Forster, D.; Hershman, A.; Morris, D. E. FR. 2,280,586, 1975.
(4) Hershman, A.; Morris, D. E.; Forster, D. (Monsanto Co.) FR 2,280,622, 1975.
(5) Forster, D. *Inorg. Chem.* **1972**, *11*, 473.
(6) Forster, D. *J. Chem. Soc., Dalton Trans.* **1979**, 1639.
(7) Roe, D. C.; Sheridan, R. E.; Bunel, E. E. *J. Am. Chem. Soc.* **1994**, *116*, 1163.
(8) Haynes, A.; Mann, B. E.; Morris, G. E.; Maitlis, P. M. *J. Am. Chem. Soc.* **1993**, *115*, 4093.
(9) Fulford, A.; Hickey, C. E.; Maitlis, P. M. *J. Organomet. Chem.* **1990**, *398*, 311.
(10) Ellis, P. R.; Pearson, J. M.; Haynes, A.; Bailey, N. A.; Maitlis, P. M. *Organometallics* **1994**, *13*, 3215.
(11) Maitlis, P. M.; Haynes, A.; Sunley, G. J.; Howard, M. J. *J. Chem. Soc., Dalton* **1996**, 2187.
(12) Wilkins, R. G. *Kinetics and Mechanism of Reactions of Transition Metal Complexes*; VCH: Weinheim, Germany, 1991.
(13) Moullet, B.; Zwahlen, C.; Frey, U.; Gervasio, G.; Merbach, A. E. *Inorg. Chim. Acta* **1997**, *261*, 67.
(14) Potgieter, J. H. *J. Organomet. Chem.* **1989**, *366*, 369.
(15) Araghizadeh, F.; Branan, D. M.; Hoffman, N. W.; Jones, J. H.; McElroy, E. A.; Miller, N. C.; Ramage, D. L.; Salazar, A. B. *Inorg. Chem.* **1988**, *27*, 3752.
(16) Garrou, P. E.; Hartwell, G. E. *Inorg. Chem.* **1976**, *15*, 646.
(17) Elmroth, S.; Skibsted, L. H.; Elding, L. I. *Inorg. Chem.* **1989**, *28*, 2703.
(18) Ventegodt, J.; Oby, B.; Skibsted, L. H. *Acta Chem. Scand.* **1985**, *39*, 453.
(19) Kaas, K.; Skibsted, L. H. *Acta Chem. Scand.* **1985**, *39*, 1.
(20) Romeo, R. *Comments Inorg. Chem.* **1990**, *11*, 21.
(21) Olsson, A.; Roodt, A.; Bojczuk, M.; Heaton, B. T.; Elding, L. I. *J. Chem. Soc., Dalton Trans.* **1994**, 3723.
(22) Wojcicki, A.; Basolo, F. *J. Am. Chem. Soc.* **1961**, *83*, 525.

10.1021/ic9910763 CCC: \$19.00

solution. This implies the utilization of specific high-pressure technologies to follow the reaction. Thus, to perform the kinetic study of CO exchange on the *cis*-$[M(CO)_2X_2]^-$ complexes (M = Rh(I), Ir(I)) presented in this paper, we have used homemade high-pressure sapphire tubes[23] to obtain dynamic ^{13}C NMR spectra under moderate CO pressures. The objective of this study was to understand the lability and the reactivity of this ligand in rhodium and iridium carbonylation chemistry.

Experimental Section

Chemicals and Solutions. Methylene chloride (CD_2Cl_2, Armar, 99.6 atom % D), *n*-hexane (Merck, >95%), carbon-13-enriched carbon monoxide (Cambridge Isotope Laboratories, 99 atom % ^{13}C), $[Ir(CO)_3Cl]_n$ (Strem Chemical, >95%), and $[Rh(CO)_2Cl]_2$ (Strem Chemical, >95%) were used without further purification.

The iridium(I) complexes *cis*-$[Ir(CO)_2X_2]P(C_6H_5)_4$ (**1a**, X = Cl; **1b**, X = Br; **1c**, X = I) were prepared using modified methods described by Forster[24] and Piraino.[25] The syntheses were carried out in an autoclave using methanol as solvent instead of 2-methoxyethanol.[24] The corresponding halide phosphonium salts, instead of arsenium salts, were used as counterions. After 1 h of reaction at 393 K, the solutions were cooled to room temperature and the solid iridium complexes were filtered off and washed with cold methanol. The rhodium(I) complexes *cis*-$[Rh(CO)_2X_2]P(C_6H_5)_4$ (**2a**, X = Cl; **2b**, X = Br; **2c**, X = I) were synthesized in two steps according to methods described in the literature.[9,26] The purities of all complexes prepared were checked by comparison of IR and NMR results to literature data.[8,27,28]

UV−Visible Measurements. Absorbance spectra were recorded on a Perkin-Elmer Lambda 19 double-beam spectrometer at 298 K between 300 and 650 nm. We used a homemade cell (optical path length ~2 cm) with magnetic stirring to increase the speed of the solution gas saturation. This cell was inserted into a pressurizable and thermostated pressure bomb.[29] The temperature was measured with a Pt resistance thermometer in the body of the bomb. A second optical cell containing CH_2Cl_2 was placed in the reference beam.

NMR Measurements. ^{13}C NMR spectra were recorded on a Bruker ARX 400 spectrometer with a narrow-bore cryomagnet (9.4 T, 100.63 MHz). The ^{13}C NMR chemical shifts, δ, are referenced to TMS and measured with respect to the solvent, CD_2Cl_2 ($\delta = 53.8$ ppm), for all the temperatures. The temperature was controlled to within ±0.2 K using a Bruker B-VT 2000 unit and was measured before and after spectral acquisition by a substitution technique with a platinum resistor.[30] We used 10 mm o.d. NMR sapphire tubes[23] (up to 6.0 MPa of ^{13}CO) for variable-[CO] and variable-temperature studies. The variable-pressure measurements to determine the activation volumes, $\Delta V^{\ddagger}$, were performed at 332.0 (**1a**) and 330.8 K (**2a**) between 0.1 and 200.0 MPa using our homemade high-pressure NMR probe.[31]

In the slow-exchange domain, the concentration of the dissolved free CO was determined by comparison of the integrated ^{13}C NMR signal of the free CO to the signal of the bound CO of *cis*-$[M(CO)_2X_2]^-$ solutions of known concentrations. In the fast-exchange domain, where only a coalesced signal is observed, we used the average chemical shift and the complex concentrations to obtain the free CO concentrations.

For quantitative NMR spectra, the different longitudinal relaxation times, T_1, of the ^{13}C NMR signals have to be known. The relaxation times, chemical shifts, multiplicities and $^2J_{^{13}C-^{109}Rh}$ coupling constants, respectively, were as follows: free dissolved CO, 2.4 s, 184.6 ppm, s; **1a**, 13.8 s, 168.6 ppm, s; **1b**, 9.4 s, 168.8 ppm, s; **1c**, 11.9 s, 170.4 ppm, s; **2a**, 13.2 s, 183.9 ppm, d, 72.1 Hz; **2b**, 8.2 s, 182.7 ppm, d, 72.4 Hz; **2c**, 11.8 s, 182.2 ppm, d, 69.0 Hz. For the kinetic determinations, all spectra were recorded under conditions where the observed rate constant was larger than 10 s^{-1}; thus the relaxation of CO was mainly governed by the relaxation in free CO. Consequently, an NMR relaxation delay of 20 s between two accumulations was used. The other parameters for the collection of ^{13}C NMR spectra were the following: frequency range 13.5−21.7 kHz; 32K−64K data points; pulse length 10 μs; exponential line broadening 1−5 Hz; number of scans 8−512. All experimental data are given in the Supporting Information.

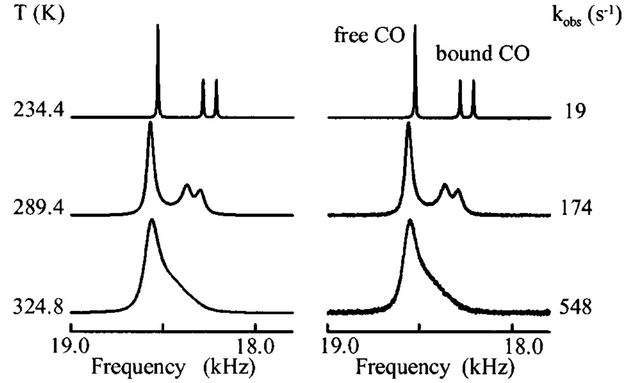

Figure 1. Calculated (left) and experimental (right) 100.63 MHz ^{13}C NMR spectra of the intermolecular exchange reaction of CO in *cis*-$[Rh(CO)_2Cl_2]^-$ (4.96×10^{-2} mol L^{-1}) in dichloromethane-d_2 solution, at variable temperatures and 2.0 MPa of ^{13}CO (~0.12 mol L^{-1}).

Data Treatment. Rate constants were obtained from line-broadened NMR spectra by least-squares fitting with the program NMRICMA[32] using the appropriate Kubo−Sack matrixes.[33] The analysis of the rate constants using the required equations was accomplished with the nonlinear least-squares fitting program Scientist.[34] The reported errors correspond to one standard deviation.

Results and Discussion

CO Exchange on *cis*-$[M(CO)_2X_2]^-$ (M = Ir, Rh; X = Cl, Br, I). At very low temperature (234.4 K), the ^{13}C NMR spectrum of **2a** in CD_2Cl_2 with a pressure of 2 MPa of ^{13}CO exhibited a doublet at 181.49 ppm corresponding to bound CO ($^2J_{^{13}C-^{109}Rh} = 72.1$ Hz) and a singlet at 184.22 ppm corresponding to free CO (Figure 1). Upon an increase in temperature, the well-separated signals of bound and free CO were broadened (289.4 K) due to an intermolecular CO exchange (eq 1) and finally coalesced (324.8 K).

$$cis\text{-}[M(CO)_2X_2]^- + 2{*}CO \xrightleftharpoons{k_{obs}} cis\text{-}[M({*}CO)_2X_2]^- + 2CO \quad (1)$$

A similar behavior (except for the absence of coupling between the iridium and bound CO) was observed for *cis*-$[Ir(CO)_2Cl_2]^-$, **1a**, and *cis*-$[Ir(CO)_2Br_2]^-$, **1b**. For the three other complexes (**1c**, **2b**, and **2c**), even at the lowest accessible temperature, only the coalesced signal of free and bound CO was observed. For complex **1c**, an additional behavior was observed: when a 10^{-2} mol L^{-1} solution in CD_2Cl_2 was pressurized with CO, the color of the solution started to change from yellow to red at a low CO pressure of 0.1 MPa, but no further color change was observed for pressures above 1.5 MPa.

---

(23) Cusanelli, A.; Frey, U.; Richens, D. T.; Merbach, A. E. *J. Am. Chem. Soc.* **1996**, *118*, 5265.

(24) Forster, D. *Inorg. Nucl. Chem. Lett.* **1969**, *5*, 433.

(25) Piraino, P.; Faraone, F.; Pietropaolo, R. *Inorg. Nucl. Chem. Lett.* **1973**, *9*, 1237.

(26) Valarino, L. M. *Inorg. Chem.* **1965**, *4*, 161.

(27) Forster, D. *Inorg. Chem.* **1969**, *8*, 2556.

(28) Forster, D. *Synth. Inorg. Met.-Org. Chem.* **1971**, *1*, 221.

(29) Richens, D. T.; Ducommun, Y.; Merbach, A. E. *J. Am. Chem. Soc.* **1987**, *109*, 603.

(30) Ammann, C.; Meier, P.; Merbach, A. E. *J. Magn. Reson.* **1982**, *46*, 319.

(31) Cusanelli, A.; Nicula-Dadci, L.; Frey, U.; Merbach, A. E. *Inorg. Chem.* **1997**, *36*, 2211.

(32) Helm, L.; Borel, A. *NMRICMA 2.03*; Lausanne University: Lausanne, Switzerland, 1998.

(33) Johnson, C.; Moreland, G. *J. Chem. Educ.* **1973**, *50*, 477.

(34) *Scientist 2.0*; MicroMath, Inc.: Salt Lake City, Utah, 1995.

When a small excess of phosphonium iodide was added, the color change was not observed and the solution remained yellow. A UV−visible spectrophotometric study (Supporting Information) confirmed these observations, suggesting the following equilibrium:

$$cis\text{-}[\mathrm{Ir(CO)_2I_2}]^- + \mathrm{CO} \overset{K}{\rightleftharpoons} [\mathrm{Ir(CO)_3I}] + \mathrm{I}^- \qquad (2)$$

The neutral complex $[\mathrm{Ir(CO)_3I}]$ and the reverse reaction have already been described by Forster using infrared spectrometry.[6] An upper limit of $K < 3 \times 10^{-4}$ for the equilibrium constant can be estimated from our UV−vis data. Therefore, in the more concentrated solution (5×10^{-2} mol L^{-1}) used in the NMR kinetic studies, less than 3% of the neutral tricarbonyl complex forms, but it is still responsible for the observed color change (see above). To check a possible influence of equilibrium 2 on the rate constant of the carbonyl exchange (eq 1), we performed a CO exchange study on *cis*-$[\mathrm{Ir(CO)_2I_2}]^-$ (3.3×10^{-2} mol L^{-1}) as a function of the free iodide concentration ($0-1.3 \times 10^{-2}$ mol L^{-1}) at 312.1 K with 9×10^{-2} mol L^{-1} dissolved CO. The rate was found to be independent of the free iodide concentration. This indicates that the red neutral tricarbonyl complex has no influence on the CO exchange kinetics. To avoid the slow formation of side products, including *cis*-$[\mathrm{Ir(CO)_2I_4}]^-$, no excess of $\mathrm{P(C_6H_5)_4I}$ was used in the NMR studies.

Variable-[CO] Studies. The general rate law for substitution on a square-planar complex consists of two terms. The first term represents the ligand substitution via the solvated complex, and the second term represents the direct nucleophilic attack of the entering nucleophile. The rate law for the present CO exchange study (eq 1) is shown in eq 3.

$$-\mathrm{d}[cis\text{-}\mathrm{M(CO)_2X_2}^-]/(\mathrm{d}t\,[cis\text{-}\mathrm{M(CO)_2X_2}^-]) = k_{\mathrm{obs}} = k_1 + k_2[\mathrm{CO}] \quad (3)$$

To study the dependence of k_{obs} on the CO concentration, the latter was varied from 0.015 to 0.50 M corresponding to pressures of 0.1−6.2 MPa. The fit of k_{obs} as a function of the CO concentration (Figure 2) indicates that the first-order rate constant, k_1, is negligible within experimental errors, and therefore, the solvent path can be neglected. Thus the observed rate constants for the CO exchange on *cis*-$[\mathrm{M(CO)_2X_2}]^-$ reduce to eq 4. The CO dependence of k_{obs} for **2c** could not be determined since the reaction is too fast under the experimental conditions required for the NMR measurements. However, it can be assumed that **2c** follows the same rate law observed for the other complexes.

$$k_{\mathrm{obs}} = k_2[\mathrm{CO}] \qquad (4)$$

The same rate law was found by Olsson et al. for CO exchange on $[\mathrm{M(CO)X_3}]^-$ complexes where M = Pd (X = Cl) or Pt (X = Cl, Br, I) in chloroform.[21]

Variable-Temperature and -Pressure Kinetics. For the variable-temperature kinetics, the temperature ranges (Table 1) were chosen as a function of the lability of the studied complexes. The rate constants were fitted using the Eyring equation (eq 5) to obtain k_2^{298} and the corresponding activation parameters, $\Delta H^\ddagger$ and $\Delta S^\ddagger$. For the same metal, the reactivity increases along the halogen series from Cl$^-$ to I$^-$, as expected from the well-known *trans* effect in square-planar complexes.[12]

$$k_2 = (k_{\mathrm{b}}T/h)\exp[(\Delta S^\ddagger/R) - (\Delta H^\ddagger/RT)] \qquad (3)$$

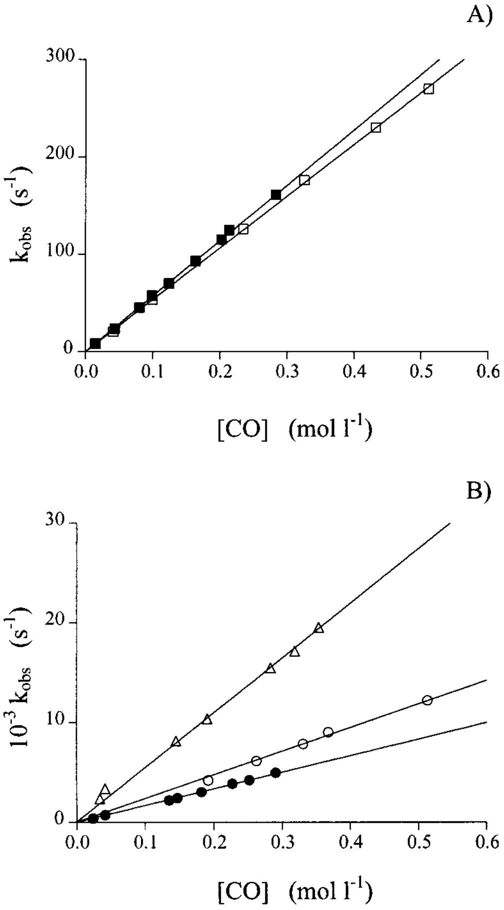

Figure 2. Observed CO exchange rate constants, k_{obs}, for *cis*-$[\mathrm{M(CO)_2X_2}]^-$ as a function of the dissolved CO concentration. (A) □: *cis*-$[\mathrm{Ir(CO)_2Cl_2}]^-$, **1a**, $T = 273.4$ K, [**1a**] = 3.91×10^{-2} mol L^{-1}. ■: *cis*-$[\mathrm{Rh(CO)_2Cl_2}]^-$, **2a**, $T = 255.1$ K, [**2a**] = 4.96×10^{-2} mol L^{-1}. (B) ○: *cis*-$[\mathrm{Ir(CO)_2Br_2}]^-$, **1b**, $T = 323.0$ K, [**1b**] = 2.20×10^{-2} mol L^{-1}. ●: *cis*-$[\mathrm{Rh(CO)_2Br_2}]^-$, **2b**, $T = 274.5$ K, [**2b**] = 4.95×10^{-2} mol L^{-1}. △: *cis*-$[\mathrm{Ir(CO)_2I_2}]^-$, **1c**, $T = 272.7$ K, [**1c**] = 4.93×10^{-2} mol L^{-1}.

Chart 1

1		15		525	for *cis*-$[\mathrm{Rh(CO)_2X_2}]^-$
Cl	<	Br	<	I	
1		12		92	for *cis*-$[\mathrm{Ir(CO)_2X_2}]^-$

A quantitative comparison of the halide effect given by the relative rate constants $k_{2\mathrm{X}}^{298}/k_{2\mathrm{Cl}}^{298}$ (X = Cl, Br, I; from Table 1) for the two metal centers is shown in Chart 1. For a given halogen, the reactivity is greater for rhodium than for iridium complexes, and their ratio, $k_{2\mathrm{X,Rh}}^{298}/k_{2\mathrm{X,Ir}}^{298}$ (from Table 1), increases also along the series 1.5, 2.0, 8.6 for Cl, Br, I.

The CO exchange rate constants for the palladium and platinum $[\mathrm{M(CO)X_3}]^-$ complexes[21] are 3−6 orders of magnitude smaller than the CO exchange rate constants for the rhodium and iridium *cis*-$[\mathrm{M(CO)_2X_2}]^-$ complexes. For $[\mathrm{Pt(CO)X_3}]^-$, a similar *trans* effect is observed with an increase of the relative rate constants 1, 18, ∼500 for Cl, Br, I. However, the second-row palladium chloro complex is 175 times more reactive than the corresponding third-row platinum analogue. In this study, we have not observed such a large reactivity difference between rhodium and iridium chloro complexes.

The enthalpy and entropy of activation, even if they are not always obvious to be obtained accurately by NMR, show very clear trends for the *cis*-$[\mathrm{M(CO)_2X_2}]^-$ family of compounds. The entropies have large negative values which together with the

Table 1. Second-Order Rate Constants, k_2^{298}, and Activation Parameters for the Free CO Exchange in Square-Planar Carbonyl Complexes in Dichloromethane

complex	temp (K)	k_2^{298} (L mol^{-1} s^{-1})	$\Delta H^\ddagger$ (kJ mol^{-1})	$\Delta S^\ddagger$ (J mol^{-1} K^{-1})	$\Delta V^\ddagger$ (cm^3 mol^{-1})	method	ref
$[Pt(CO)Cl_3]^-$ [a]	288−308	$(3.3 \pm 0.3) \times 10^{-3}$	60 ± 7	−91 ± 22		IR, NMR[b]	21
$[Pt(CO)Br_3]^-$	293−303	$(6.0 \pm 0.2) \times 10^{-2}$	49 ± 6	−104 ± 19		IR	21
$[Pt(CO)I_3]^-$	298	>2				IR	21
$[Pd(CO)Cl_3]^-$	248−368	0.57 ± 0.07	60 ± 8	−47 ± 30		NMR	21
$[Pt_2(CO)_2Cl_4]$	291	>10[c]				^{14}C[d,e]	22
$[Rh_2(CO)_4Cl_2]$	273	>10[c]				^{14}C[d]	22
$[Rh(P(C_6H_5)_3)_2(CO)Cl]^-$	273	>10[c]				^{14}C[d]	22
cis-$[Ir(CO)_2Cl_2]^-$, **1a**	247−332	$(1.08 \pm 0.01) \times 10^3$ [f]	15.37 ± 0.3	−135.3 ± 1	−20.9 ± 1.2[g]	NMR	*h*
cis-$[Ir(CO)_2Br_2]^-$, **1b**	243−329	$(12.7 \pm 0.2) \times 10^3$ [f]	13.26 ± 0.5	−121.9 ± 2		NMR	*h*
cis-$[Ir(CO)_2I_2]^-$, **1c**	255−314	$(98.9 \pm 1.4) \times 10^3$ [f]	12.50 ± 0.6	−107.4 ± 2		NMR	*h*
cis-$[Rh(CO)_2Cl_2]^-$, **2a**	234−325	$(1.62 \pm 0.02) \times 10^3$ [f]	17.47 ± 0.4	−124.9 ± 1	−17.2 ± 1.0[i]	NMR	*h*
cis-$[Rh(CO)_2Br_2]^-$, **2b**	274−313	$(24.8 \pm 0.2) \times 10^3$ [f]	11.35 ± 0.4	−122.7 ± 1		NMR	*h*
cis-$[Rh(CO)_2I_2]^-$, **2c**	195−224	$(850 \pm 120) \times 10^3$ [f,j]	9.87 ± 0.8	−98.3 ± 4		NMR	*h*

[a] IR and NMR data fitted simultaneously. [b] NMR in chloroform. [c] Estimation. [d] Radioactive isotopic exchange in chloroform. [e] In benzene. [f] The k_2 and $\Delta S^\ddagger$ values refer to the exchange of one particular CO molecule. The exchange rate constant for the exchange of either of the two coordinated CO molecules is 2 times larger. [g] $T = 332.0$ K. [h] This work. [i] $T = 330.8$ K. [j] Extrapolation at 298 K.

Table 2. Experimental CO Exchange Rate Constants for *cis*-$[M(CO)_2Cl_2]^-$ (M = Ir, Rh) as a Function of Pressure in CD_2Cl_2 with an Ambient Pressure ^{13}CO Saturated Solution (≤0.01 mol L^{-1})

cis-$[Ir(CO)_2Cl_2]^-$, **1a**[a]		*cis*-$[Rh(CO)_2Cl_2]^-$, **2a**[b]	
P (MPa)	k_{obs} (s^{-1})	*P* (MPa)	k_{obs} (s^{-1})
8.3	16	4.3	23
33.5	22	5.4	25
73.8	30	27.4	28
120.1	41	50.2	40
140.3	44	73.8	40
161.3	50	102.0	50
196.0	75	123.6	54
		151.6	62
		174.3	72
		197.3	82

[a] 8.48×10^{-3} mol L^{-1}; $T = 332.0$ K. [b] 9.29×10^{-3} mol L^{-1}; $T = 330.8$ K.

observed second-order rate laws confirm the assignment of an associative activation mode.

In recent work, the activation volume, $\Delta V^\ddagger$, was successfully used for the assignment of inorganic substitution mechanisms,[35] in particular for exchange reactions.[36] For technical reasons, the activation volume is difficult to measure for these CO exchange reactions. In fact, the samples have to be prepared at ambient pressure, and therefore, only a small CO concentration (ca. 0.01 M) can be obtained. Under these dilute conditions, good signal-to-noise ratios can only be obtained in the slow-exchange NMR region, where the data analysis is highly simplified. Hence, the high-pressure study was limited to the two chloride complexes **1a** and **2a**. The half-widths of the ^{13}C signal of bound CO, $w_{1/2}$, are directly related to the observed exchange rates, $k_{obs} = w_{1/2}\pi$. These values (Table 2) were adjusted to eq 6, where $k_{obs,0}$ is

$$\ln(k_{obs}) = \ln(k_{obs,0}) - (\Delta V^\ddagger P/RT) \qquad (6)$$

the observed rate constant at ambient pressure. The fit resulted in $\Delta V^\ddagger = -20.9 \pm 1.2$ cm^3 mol^{-1} for **1a** and -17.2 ± 1.0 cm^3 mol^{-1} for **2a**. These are the first values for CO exchange in square-planar species, which limits any possible comparison. For homoleptic square-planar MS_4^{2+} complexes reacting via associative mechanisms, the third-row platinum complexes ($\Delta V^\ddagger$ (cm^3 mol^{-1}): H_2O, −4.6; Me_2S, −22.0) show more negative activation volumes than the second-row palladium analogues (S, $\Delta V^\ddagger$ (cm^3 mol^{-1}): H_2O, −2.2; Me_2S, −9.4).[35,36] This trend is also observed for the iridium(I) and rhodium(I) dichloro dicarbonyl complexes.

Conclusions

In this work, we report the first activation volumes for a CO exchange reaction on square-planar complexes. The rate of this exchange reaction increases along the halide series (Cl^- to I^-) according to the *trans* effect and is faster for the rhodium than for the iridium complexes for a given halide. The activation volumes, $\Delta V^\ddagger$, which are among the most negative values found for ligand exchange reactions in square-planar complexes, and the large negative $\Delta S^\ddagger$ values, obtained from the variable-pressure and temperature studies, as well as the second-order rate law, are all consistent with an associative activation mode and point to a limiting A mechanism.

Acknowledgment. The authors thank Rhône-Poulenc and the Swiss National Science Foundation for financial support.

Supporting Information Available: Influence of free iodide concentration on the observed rate constant, k_{obs}, for CO exchange on *cis*-$[Ir(CO)_2I_2]^-$ (Table S1), ^{13}C NMR chemical shifts of CO as a function of temperature in CD_2Cl_2 for free CO (Figure S1 and Table S2) and bound CO in *cis*-$[M(CO)_2X_2]^-$ (Figure S2 and Table S2), Kubo−Sack matrixes for CO exchange on *cis*-$[Ir(CO)_2X_2]^-$ (X = Cl, Br, I; Figure S3) and on *cis*-$[Rh(CO)_2X_2]^-$ (X = Cl, Br, I; Figure S4), UV−visible spectra of *cis*-$[Ir(CO)_2I_2]^-$, **1c**, obtained with and without added $P(C_6H_5)_4I$ under different CO pressures (Figure S5), Eyring plots of the second-order rate constant, k_2, for CO exchange in *cis*-$[M(CO)_2X_2]^-$ (M = Ir, Rh; X = Cl, Br, I) in CD_2Cl_2 (Figure S6), longitudinal relaxation times, T_1, for free CO and bound CO on *cis*-$[M(CO)_2X_2]^-$ complexes at ambient temperature (M = Rh, Ir; X = Cl, Br, I; Table S3), rate constants for CO exchange on *cis*-$[M(CO)_2X_2]^-$ (M = Rh, Ir; X = Cl, Br, I) in CD_2Cl_2 as a function of CO concentration (Table S4) and as a function of temperature (Table S5) and a plot of k_2 as a function of pressure (Figure S7). This material is available free of charge via the Internet at http://pubs.acs.org.

IC9910763

---

(35) Drljaca, A.; Hubard, C. D.; van Eldik, R.; Asano, T.; Basilevsky, M. V.; Le Noble, W. J. *Chem. Rev.* **1998**, *98*, 2167.

(36) Lincoln, S. F.; Merbach, A. E. *Adv. Inorg. Chem.* **1995**, *42*, 1.